Experiments and Considerations on Reaction-Diffusion based Pattern Generation in a Wireless Sensor Network

Katsuya Hyodo, Naoki Wakamiya, Etsushi Nakaguchi, Masayuki Murata
Graduate School of Information Science and Technology, Osaka University
1-5 Yamadaoka, Suita, Osaka 565-0871, Japan
{k-hyodo, wakamiya, nakaguti, murata}@ist.osaka-u.ac.jp

Yuki Kubo, Kentaro Yanagihara
Corporate Research & Development Center, Oki Electric Industry Co.,Ltd
2-5-7 Honmachi, Chuo-ku, Osaka, Osaka 541-0053, Japan
{kubo635, yanagihara726}@oki.com

Abstract

Taking into account requirements of sensor networks, we need fully-distributed and self-organizing control mechanisms which are scalable to the size of a network, robust to failures of sensor nodes, and adaptive to different and dynamically changing topology and changes in wireless communication environment. To accomplish this goal, our research group focuses on behavior of biological systems, which inherently are scalable, adaptive, and robust. In this paper, we first verify the practicality of control mechanisms adopting a reaction diffusion equation, which explains emergence of patterns on the surface of body of fishes and mammals, and then propose two methods for faster pattern generation to save energy consumption. From simulation and practical experiments on a prototype, it was shown that a stable pattern could be generated in a wireless sensor network in several minutes, even when packets were lost for collisions in wireless communication.

1 Introduction

Wireless sensor network is one of the most promising and key technologies for safe, secure, and comfortable society. By distributing a large number of sensor nodes and organizing a network through wired / wireless communication, one can obtain detailed information about surroundings, remote region, entities, and objects. Because of a large number of sensor nodes, random or unplanned deployment, and dynamic topology changes due to addition, movement, and removal of sensor nodes, control mechanisms for a wireless sensor network must be scalable, adaptive, and robust. In addition, due to difficulty in managing a large number of nodes in a centralized fashion, mechanisms must be fully distributed and self-organizing.

To establish control mechanisms with the above mentioned features, we focus on behavior of biological systems, which inherently are scalable, adaptive, and robust. For example, in [1], we applied a pulse-coupled oscillator model, which explains emergence of synchronized behaviors in a group of flashing fireflies and chirping crickets, to energy-efficient data gathering. Other examples of biological mechanisms applicable to sensor networks include foraging behavior of ants [2, 3] and bees [4], regulation of blood pressure [5], and so on.

A reaction-diffusion equation is also viable as a key algorithm for autonomous control mechanisms. It was firstly proposed by Alan Turing [6] as a mathematical model for pattern generation on the surface of body of fishes and mammals. Autonomously generated patterns on a sensor network can be used for routing, clustering, scheduling, and topology control. There are some researches adopting a reaction-diffusion equation to establish an autonomous and self-organizing mechanism [7–9]. For example, RDMAC [8] is a reaction-diffusion based MAC protocol, where they noticed the similarity among a scheduling pattern of spatial TDMA and a spot pattern of leopards. A node inhibits packet emission of neighboring nodes in its range of radio signals while encouraging nodes out of the range to send packets for better spatial use of a wireless channel.

Although these works show the potential applicability of a reaction-diffusion equation to a control mechanism of a wireless sensor network, they only evaluated the proposal

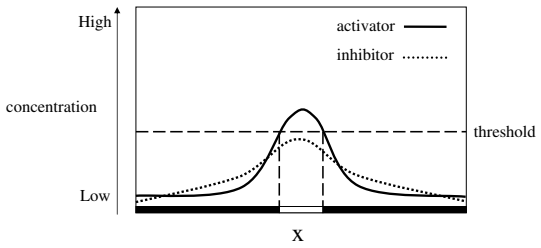

Figure 1. Pattern generation

through simulation experiments under ideal condition. In this paper, we conducts both of simulation and practical experiments to verify the practicality of reaction-diffusion based pattern generation. In addition, to have an energy-efficient control, we propose two methods to reduce the number of message exchanges required for pattern generation. We further evaluate the influence of packet loss considering a practical scenario.

The rest of the paper is organized as follows. In Section 2, we introduce a reaction-diffusion equation that our paper is based on. Next in Section 3, we describe our reaction-diffusion based control mechanism for a wireless sensor network. In Section 4, we then show and discuss results of simulation and practical experiments. Finally, we conclude the paper in Section 5.

2 Reaction-diffusion equation

A reaction-diffusion equation of two morphogens, i.e., activator and inhibitor, can be written as

$$\begin{cases} \dfrac{\partial u}{\partial t} = F(u,v) + D_u \nabla^2 u, \\ \dfrac{\partial v}{\partial t} = G(u,v) + D_v \nabla^2 v, \end{cases} \tag{1}$$

where u and v are the concentrations of activator and inhibitor, respectively. The first term of the right-hand side is a reaction team and the second term is a diffusion term. F and G are nonlinear functions for chemical reactions. D_u and D_v are the diffusion rate of activator and inhibitor, respectively. ∇^2 is the Laplacian operator.

In a reaction-diffusion mechanism, the following conditions must be satisfied to generate patterns; 1) The activator activates itself and the inhibitor, whereas the inhibitor restraints the activator, and 2) The inhibitor diffuses faster than the activator ($D_v > D_u$). A mechanism of pattern generation can be explained as follows. In Fig. 1, those hypothetical chemicals are arranged in a line on the x-axis. The y-axis corresponds to the concentrations of activator and inhibitor. Now, consider that the concentration of activator has a peak at the center by a slight perturbation. The concentrations of activator and inhibitor are increased around the peak by self-activation. The generated inhibitor diffuses faster than the activator and restrains generation of activator at further regions. On the other hand at the peak, the concentration of activator is kept higher than that of inhibitor for different rates of diffusion. Consequently, the diversity in the concentration of activator emerges and a pattern appears. For example, when we color a point where the concentration of activator exceeds a certain threshold with white and others with black, we can see a black-white-black pattern shown at the bottom of Fig. 1.

In this paper, we use the equations below for F and G, which model pattern generation on an emperor angelfish *pomacanthus imperator* [10].

$$\begin{cases} F(u,v) = \max\{0, \min\{au - bv + c, M\}\} - du, \\ G(u,v) = \max\{0, \min\{eu + f, N\}\} - gv, \end{cases} \tag{2}$$

where a and e correspond to the rate of activation and b is for that of inhibition. c and f are parameters for synthesis or increase of morphogens per unit time. d and g are for decomposition or decrease of morphogens per unit time. M and N are constants of limit. In order to generate patterns, the parameters must satisfy Turing conditions shown below.

$$a - d - g < 0, \tag{3}$$

$$eb - (a-d)g > 0, \tag{4}$$

$$D_v(a-d) - D_u g > 0, \tag{5}$$

$$(D_v(a-d) - D_u g)^2 - 4D_u D_v(eb - (a-d)g) > 0. \tag{6}$$

As far as these conditions are satisfied, the space will have the spatial heterogeneity in terms of the concentration of morphogens and a variety of patterns such as spots, stripes, and maze can be generated.

If the initial concentrations of activator and inhibitor are both larger than zero, u and v have the upper limit $u_{max} = r/d$ and $v_{max} = s/g$, respectively. The lower limits are $u_{min} = v_{min} = 0$. Although the derivation is not shown in the paper due to the space limitation, by regarding $F(u,v)$ as $(a-d)u - bv + c$ and $G(u,v)$ as $eu - gv + f$, wavelength l of a generated pattern can be derived as,

$$l = 2\pi \sqrt[4]{\frac{D_u D_v}{eb - (a-d)g}}. \tag{7}$$

3 Reaction-diffusion based control mechanism

To verify the practicality of a reaction-diffusion based mechanism, we consider a simple and general mechanism described as follows.

Nodes are arranged in a grid network topology, where a node can communicate with four direct neighbors in up, right, down, and left directions. Nodes at a corner have two neighbors and nodes at an edge have three neighbors. At regular intervals, a node calculates the reaction-diffusion equation by using information about morphogen concentrations of neighbors, which it has received after the previous control timing. Then, it broadcasts information about its morphogen concentrations to the neighbors. If a node did not receive concentration information from a neighbor in this interval, it uses the latest information it received instead. Nodes behave in an asynchronous manner. It means that timing of message emission and reaction-diffusion calculation are different among nodes.

Since the arrangement of nodes and exchange of information are discrete in space and time, we first discretize Eq. (1) as follows.

$$\begin{aligned} u_{t+1} &= u_t + \Delta t \\ &\left\{ F(u_t, v_t) + D_u \frac{(u_t^n + u_t^e + u_t^s + u_t^w - 4u_t)}{\Delta h^2} \right\}, \\ v_{t+1} &= v_t + \Delta t \\ &\left\{ G(u_t, v_t) + D_v \frac{(v_t^n + v_t^e + v_t^s + v_t^w - 4v_t)}{\Delta h^2} \right\}. \end{aligned} \tag{8}$$

At the t-th control timing, a node calculates the reaction-diffusion equation to obtain its morphogen concentrations u_{t+1} and v_{t+1}, based on which a node decides its behavior, e.g., color, in the next control interval. A set of u_t^n, u_t^e, u_t^s, and u_t^w and a set of v_t^n, v_t^e, v_t^s, and v_t^w correspond to neighboring nodes' concentrations of activator and inhibitor that a node uses for calculation at the t-th control timing, respectively. Δh and Δt correspond to the distance between nodes and the discrete step interval of time, respectively. There is the range of Δt for the equation reaches convergence,

$$\begin{aligned} 0 < \Delta t < \min\Big\{ & \frac{2}{d + 4D_u(\Delta x^{-2} + \Delta y^{-2})}, \\ & \frac{2}{g + 4D_v(\Delta x^{-2} + \Delta y^{-2})} \Big\}. \end{aligned} \tag{9}$$

As far as the degree of temporal discretization is within this range, the same pattern is generated for the same set of parameters.

Since a sensor node has the limited computational capability, integer arithmetic is preferred for high speed operation. However, integer arithmetic introduces several problems such as truncation error, cancellation error, loss of trailing digit, and overflow. When the number of significant digits is insufficient, a generated pattern becomes different from that obtained by real number computation or a pattern does not converge. In this paper, we set the number of significant digits as four. Since concentrations of activator and inhibitor range from 0 to M and N and they are set at 0.2 and 0.5, respectively, we multiply the concentrations by 10^3 to have four-significant-digit numbers. We confirmed this was sufficient from simulation experiments.

Table 1. Parameter setting

parameter	value	parameter	value
a'	80	D'_u	2
b'	80	D'_v	50
c'	20	M'	200000
d'	30	N'	500000
e'	100	ΔT	1
f'	-150	Δh	1
g'	60		

Taking into account this, we use the following equations in place of Eqs. (2) and (8).

$$\begin{aligned} 10^4 \times u'_{t+1} &= 10^4 \times u'_t + \Delta T \Big\{ F'(u'_t, v'_t) \\ &\quad + D'_u \frac{u_t^{n\prime} + u_t^{e\prime} + u_t^{s\prime} + u_t^{w\prime} - 4u'_t}{\Delta h^2} \Big\}, \\ 10^4 \times v'_{t+1} &= 10^4 \times v'_t + \Delta T \Big\{ G'(u'_t, v'_t) \\ &\quad + D'_v \frac{v_t^{n\prime} + v_t^{e\prime} + v_t^{s\prime} + v_t^{w\prime} - 4v'_t}{\Delta h^2} \Big\}, \end{aligned} \tag{10}$$

and

$$\begin{aligned} F'(u'_t, v'_t) &= \\ &\max\big\{0, \min\big\{a'u'_t - b'v'_t + c', M'\big\}\big\} - d'u'_t, \\ G'(u'_t, v'_t) &= \\ &\max\big\{0, \min\big\{e'u'_t + f', N'\big\}\big\} - g'v'_t, \end{aligned} \tag{11}$$

where parameters with prime are multiples of corresponding parameters by 10^3 except that M' and N' are multiples of M and N by 10^6, respectively. ΔT is a multiple of Δt by 10.

4 Simulation and practical experiments

In this section, we show results of simulation and practical experiments and discuss the practicality and applicability of the reaction-diffusion based mechanism.

4.1 Simulation experiments

First, we verify the appropriateness of our spatial discretization of the reaction-diffusion equation. Basic parameters are summarized in Table 1, which satisfy the Turing conditions. Nodes are arranged in a 100×100 grid network. At the beginning of a simulation run, the concentrations of activator and inhibitor of the node at (50,50) are set

Figure 2. Comparison of simulation and analysis: wavelength

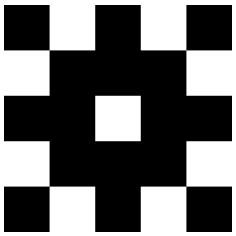

Figure 3. Generated pattern by simulation

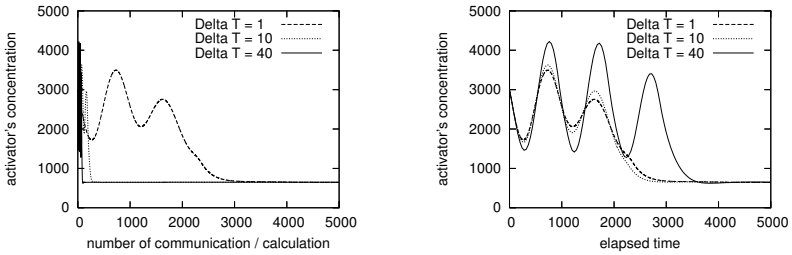

Figure 4. Simulation result of method (a)

at 5000 and 3000, respectively. The concentrations at the other nodes are all set at 3000. Some results of comparison among simulation and analysis is illustrated in Fig. 2 for the wavelength of generated patterns. The wavelength of a pattern generated by simulation is obtained by averaging the sum of widths of black and white stripes over stripes. As shown in the figures, the results match among simulation and analysis. With the finer spatial discretization with a smaller Δh, results become closer. We also evaluated the upper limit of temporal discretization ΔT and simulation and analysis had good matches, but results are not shown in the paper due to the space limitation.

Figure 3 illustrates a stable pattern generated on a 5×5 grid network with a set of parameters in Table 1. A white square corresponds to a node with the concentration of activator higher than 3000. A black square is for a node with the concentration of activator smaller than 3000. Since we set a peak of the concentration of activator at the center, a generated pattern forms concentric circles.

Pattern generation normally takes time and requires a considerable number of calculations. It further corresponds to the number of communication and the energy consumption. Therefore, we need to accelerate pattern generation for energy-efficient and adaptive controls. We propose two methods, (a) to have a larger discrete step ΔT and (b) to calculate the reaction-diffusion equation for K times at each control timing.

Figure 4 show results of changing ΔT to 1, 10, and 40 by using the method (a). The other parameters are set based on Table 1. The theoretical upper limit of ΔT is 43.5. Generated patterns are the same among all. The left figure of Fig. 4 illustrates the transition of concentration of activator at the node at the upper left corner against the number of communication and calculations. The number of communication corresponds to the number of messages that a node emits and it is equivalent to the number of control intervals. Since a node calculates the reaction-diffusion equation once per control interval, the number of communication and the number of calculations are identical for the method (a). As shown in the left figure of Fig. 4, the number of communication and calculations required for the convergence of concentration of activator can be decreased by increasing ΔT. However, the faster convergence is achieved at the sacrifice of the accuracy of calculation. The right figure of Fig. 4 shows the transition of concentration of activator against the elapsed time in reaction diffusion calculation. The elapsed time is derived by multiplying ΔT by the number of communication or calculations. We can see that a larger ΔT leads to larger fluctuation, because the accuracy of calculation becomes lower with a larger ΔT for discretization. However, in our simulation experiments, all ΔT within the range of Eq. (9) result in the same stable pattern illustrated in Fig. 3.

Next, we evaluate the method (b). Figure 5 shows results of changing K as 1, 10, and 40. The other parameters are set as Table 1. Generated patterns are the same among all independently of K. In the case of the method (b), at regular control timing, a node calculates the reaction-

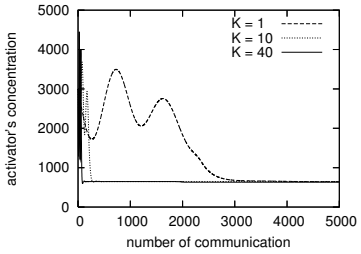

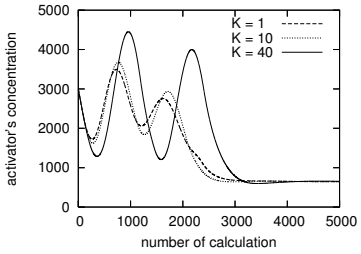

Figure 5. Simulation result of method (b)

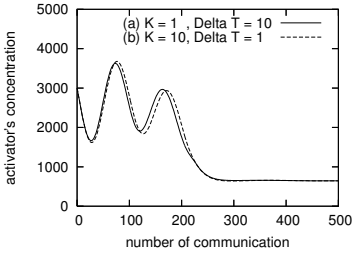

Figure 6. Comparison among methods

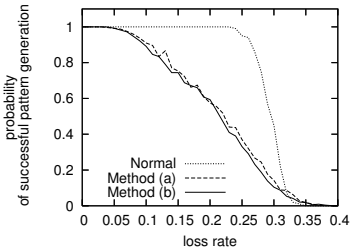

Figure 7. Influence of information loss

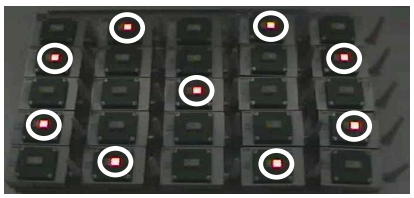

Figure 8. Prototype

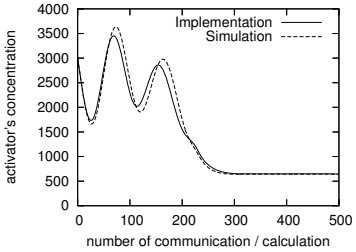

Figure 9. Comparison among simulation and implementation

diffusion equation for K times by using the same concentration values for neighboring nodes, and then broadcasts the result. Therefore, the number of calculations is K times larger than the number of communication. In the left figure of Fig. 5, the transition of concentration of activator is depicted against the number of communication for different setting of K. As shown, a larger K decreases the number of communication required for convergence. Since a larger K spoils the accuracy of reaction-diffusion calculation as a larger ΔT does, the transitions of concentration of activator against the number of communication are similar among the right figures of Fig. 4 and Fig. 5. K also has the limitation on the effective range to generate a pattern. When K is greater than 130, the concentration of activator does not converge and a pattern becomes unstable. In the range of $40 < K < 130$, the number of communication required to reach a stable pattern does not change. Therefore, the effective range of K is from 0 to 40. Figure 6 illustrates comparison among the methods, where $K = 1$ and $\Delta T = 10$ for the method (a) and $K = 10$ and $\Delta T = 1$ for the method (b). As shown in the figure, those methods show quite similar behavior.

Although the proposed methods can effectively reduce the number of communication, it sacrifices the robustness against information loss. Figure 7 shows the probability of successful pattern generation against the information loss rate. We assume that the information about concentrations is lost at random at the information loss rate. The probability of successful pattern generation is defined as the ratio of simulation runs which reach the same stable pattern that is generated for the case without loss of information to all 1000 simulation runs. As shown in Fig. 7, our acceleration methods can generate a stable pattern under random information loss of 4%, whereas a normal mechanism without acceleration can tolerate up to 23% random information loss. Therefore, we need an additional mechanism, such as retransmission, to generate patterns under unstable and unreliable radio conditions.

4.2 Practical experiments

We implement the reaction-diffusion based mechanism using off-the-shelf nodes of OKI Electric Industry (Fig. 8). We added a board with large LEDs for better visualization of pattern generation. 25 nodes are arranged in a 5×5 grid network. All nodes use the same reaction-diffusion equation of the same parameter setting in Table 1 and adopt the method (a) with $\Delta T = 10$. A node uses IEEE 802.15.4 non-beacon mode MAC protocol. 32 bit signed integer is used for calculation. All nodes are in the range of radio signals of each other. Therefore, to restrict nodes to communicate among direct neighbors, we introduce a MAC address-

based filter. A node maintains a list of MAC addresses of neighboring nodes to communicate with, and it only receives packets originated from nodes in the list. A packet broadcast by a node is of 32 bytes including a header, the concentrations of activator and inhibitor, the total number of calculations it has conducted, and the total number of packets it has not received. The last two are for logging and debugging purpose.

We determine the control interval to keep the average loss rate less than 4%. If the control interval is too short, nodes behave in synchrony and the loss rate becomes high for collision and congestion. We conducted preliminary experiments by changing the control interval and found that the control interval must be larger than about 700 msec to keep the loss rate below 4%. Therefore, we empirically set the control interval as 1400 msec taking into account dynamic changes in wireless communication environment.

In Fig. 8, nodes with a LED on are indicated by circles. A node turns on its LED when the concentration of activator is higher than 3000. In comparison to Fig. 3, it is verified that the prototype can generate the same pattern as in simulation. Figure 9 shows the detailed comparison. There is no loss of information in simulation, whereas the average packet loss rate is about 3% on the prototype. Nevertheless, transitions of concentration of activator are almost the same among the prototype and simulation. Therefore, We can conclude that the reaction-diffusion based pattern generation works on an actual wireless sensor network and the number of communication, i.e., the amount of energy consumption, can be reduced by our acceleration methods with appropriately chosen parameters.

5 Conclusion

In this paper, we verified the practicality of reaction-diffusion based control mechanisms for wireless sensor networks by simulation and practical experiments. We also proposed two method to accelerate pattern generation for energy-efficiency. We plan to consider a system which can generate an application-oriented pattern under conditions of random node layout, dynamic changes in topology, and a larger number of nodes.

Acknowledgement

This work was partly supported by "Special Coordination Funds for Promoting Science and Technology: *Yuragi Project*", Grant-in-Aid for Scientific Research on Priority Areas 18049050, and a Grant-in-Aid for Scientific Research (A)(2) 16200003 of the Ministry of Education, Culture, Sports, Science and Technology in Japan.

References

[1] N. Wakamiya and M. Murata, "Synchronization-based Data Gathering Scheme for Sensor Networks," *IEICE Transaction on Communications, Special Section on Ubiquitous Networks*, vol. E88-B, pp. 873–881, Mar. 2005.

[2] R. Huang, J. Zhu, X. Yu, and G. Xu, "The Ant-Based Algorithm for the Optimal Many-to-one Routing in Sensor Networks," in *Proceedings of International Conference on Communications, Circuits and Systems 2006*, vol. 3, Jun. 2006, pp. 1532–1536.

[3] S. Selvakennedy, S. Sinnappann, and Y. Shang, "T-ANT: A Nature-Inspired Data Gathering Protocol for Wireless Sensor Networks," *JOURNAL OF COMMUNICATIONS (JCM)*, vol. 1, issue 2, pp. 22–29, May 2006.

[4] P. Boonma and J. Suzuki, "Biologically-Inspired Data Aggregation for Multi-Modal Wireless Sensor Networks," in *Proceedings of the 31st IEEE Conference on Local Computer Networks*, Nov. 2006.

[5] F. Dressler, "Bio-inspired Promoters and Inhibitors for Self-Organized Network Security Facilities," in *Proceedings of 1st IEEE/ACM International Conference on Bio-Inspired Models of Network*, Dec. 2006.

[6] A. M. Turing, "The Chemical Basis of Morphogenesis," *Royal Society of London Philosophical Transactions Series B*, vol. 237, pp. 37–72, Aug. 1952.

[7] Y. Chen and T. C. Henderson, "S-nets: Smart Sensor Networks," in *Proceedings of International Symposium on Experimental Robotics*, Dec. 2000, pp. 85–94.

[8] M. Durvy and P. Thiran, "Reaction-Diffusion Based Transmission Patterns for Ad Hoc Networks," in *Proceedings of IEEE INFOCOM 2005*, vol. 3, Mar. 2005, pp. 2195–2205.

[9] A. Yoshida, K. Aoki, and S. Araki, "Cooperative Control Based on Reaction-Diffusion Equation for Surveillance System." in *Proceedings of Ninth International Conference on Knowledge-Based Intelligent Information and Engineering Systems*, Sep. 2005, pp. 533–539.

[10] S. Kondo and R. Asai, "A Reaction-Diffusion Wave on the Kin of the Marine Angelfish Pomacanthus," *Nature*, vol. 376, pp. 765–768, Aug. 1995.